Chiang Mai J. Sci. 2018; 45(2) : 973-983
http://epg.science.cmu.ac.th/ejournal/
Contributed Paper

The Study of Activity and Selectivity of Calcium Oxide Nanocatalyst for Transesterification of High Free Fatty Acid Crude Palm Oil

Rattana Thaoklua, Jaroon Janjaroen and Karaked Tedsree*
Nanocatalysis Laboratory, Department of Chemistry, Faculty of Science, Burapha University,
Chonburi 20131, Thailand.
* Author for correspondence; e-mail: karaked@buu.ac.th

Received: 17 June 2016
Accepted: 12 November 2016

ABSTRACT

Nanoscale CaO was demonstrated as a high activity and selectivity catalyst for transesterification of crude palm oil. The CaO catalyst with particle sizes diameter of 12±4 nm and specific surface areas 70 m^2g^{-1} was synthesized by sol-gel process. Photoluminesence spectra clearly demonstrated high number of oxide ions at low coordination sites (edges and corners) of nano CaO. FT-IR spectra showed that oxide ions at low coordination sites can accelerate deprotonation of methanol and glycerol at room temperature. Highly reactive calcium methoxide and calcium glyceroxide species were formed at room temperature leading to high reaction kinetic of transesterification. A high yield of fatty acid methyl esters (% FAME) of 98% was achieved within 30 min with 2.0 wt% of nano CaO catalyst. High formation of calcium methoxide at room temperature leads to high selectivity of transesterification leading to decrease in the level of calcium soap from saponification of free fatty acid. These active species promote transesterification in the forward direction, increasing the rate of conversion and reduction of soap formation.

Keywords: nano CaO, transesterification, crude palm oil

1. INTRODUCTION

Biodiesel is an alternative fuel derived from renewable resources, such as vegetable oils and animal fats. The method commonly used to produce biodiesel is transesterification of triglyceride (the main composition of oils) with methanol in the presence of strong acidic or basic catalysts [1]. The most catalyst used in biodiesel production is homogeneous alkaline bases such as NaOH and KOH [2-3]. However, a number of heterogeneous base catalysts, such as alkaline earth oxides and hydroxides, have been intensively investigated due to their many advantages [4]. They are noncorrosive, environmentally benign, can easier to separate from the product and can be designed to give high activity and selectivity. Among the alkaline earth oxides, calcium oxide (CaO) is a promising solid catalyst for biodiesel production as it has strong basicity, lower solubility and economically benign [5, 6]. However, its use is still limited to industrial applications due to many aspects such as mass transfer resistant, time consuming, inefficient catalytic activity and formation of CaO soap. Using nanoscale CaO with high specific surface area and surface-dependent properties is proposed as a promising way to solve the problems [7].

There have been some reports on using nanocatalyst for biodiesel production. Isahak and co-workers studied transesterification of palm oil using nano CaO catalyst [8]. This catalyst demonstrated high biodiesel conversion with low formation of soap and emulsion. Zhao and co-workers studied transesterification of canola oil by two types of commercial CaO; high surface area (HSA nano CaO, surface area = 89.52 m^2/g) and moderate surface area (nano CaO, surface area = 22.25 m^2/g). The results revealed that HSA nano CaO possess high catalytic activity than nano CaO more than 10 times due to their larger BET surface areas. The biodiesel yield (%FAME) was achieved to 99.85% within 2 h using 3 wt. % of the HAS nano CaO catalyst. These clearly confirm that the particle size and surface areas of nano CaO play an important role in the conversion yield [9]. Reddy and co-workers demonstrated that biodiesel can be produced by using nanocrystalline CaO under room-temperature. However, the reaction rate was slow and it required 6-24 h to obtain high conversion [10]. Some studies have shown that high specific surface areas and large porosity are beneficial for the catalysts to bond with the sub-layer which enhances the efficiency of transesterification reaction [11]. Thus, not only properties of CaO catalyst but also properties of oil feedstock play a significant role in determining the production yield and properties of biodiesel. There has been known that the properties of biodiesel depend on their contents of fats and acidity in oil feedstock. Low-cost feedstock such as crude palm oil (CPO) is normally contains high free fatty acid which too far beyond the level that could be converted into biodiesel by transesterification reaction. Acid catalyzed pre-treatment step by esterification reaction to convert free fatty acid to fatty acid methyl ester is required before transesterification with alkali–catalyzed process [12]. However, the employment of different catalysts and equipments for the separated processes could increase the cost for large-scale biodiesel production. Since, biodiesel from food-grade oils is not economically competitive with petroleum-based diesel fuel, lower-cost feedstock are required. However, biodiesel production from high free fatty acid of crude palm oil under base-catalyzed reaction is quite challenged because of the competition between transesterification, which is the desired path and saponification reaction, which produces undesirable soap [13]. This work we aim to develop CaO catalyst for producing quality biodiesel from crude palm oil in single step process. High surface areas of unsaturated sites (edges and coners) and size-dependent properties of nano CaO was found not only enhance the catalytic activity but also catalytic selectivity toward transesterification of triglyceride.

2. MATERIALS AND METHODS

2.1 Materials

Crude palm oil contained 12% of free fatty acid and 1% of moisture was used as a feedstock. Calcium nitrate tetrahydrate ($Ca(NO_3)_2.4H_2O$) was purchased from Loba Chmie. Polyvinyl (pyrolidone PVP) 40,000 MW was purchased from Sigma Aldrich. Methanol was dried over Type 3A molecular sieve before using. Laboratory-grade CaO was prepared by calcination of $CaCO_3$ from lime at 800°C for 4 h.

2.2 Preparation of CaO Nanoparticles (Nano CaO)

Nano CaO was prepared following the procedure described in the literature with some modifications [14]. Typically, 100 ml of ethylene glycol was heated in a three-neck round-bottom flask at 120°C in an oil bath for half an hour, then 48 g of $Ca(NO_3)_2$ and 6.5 g of PVP were introduced into the flask. After the mixture was homogeneously dissolved, 48 ml of 4.3 M aqueous solution of NaOH was added drop by drop at 3 mL/min, into the mixture. The mixture was vigorously stirred at the same temperature for 30 min. The obtained gel was kept for about 10 min in static state and allows it to cool to room temperature. The product was separated by hot vacuum filtration. Then, the particles were dispersed in 2-propanol in an ultrasonic bath and separated by centrifugation at 4,500 rpm for 5 min. The white powder was dried in air at 120°C for 4 h and calcined at 700°C for 4 h and then kept under nitrogen atmosphere.

2.3 Characterization

X-ray diffraction patterns were recorded on a Bruker AXS D8 Advance X-ray powder diffractometer using Cu-Kα radiation as an X-Ray source. Transmission electron microscope (TEM) was conducted on a TECNAI 20 microscope operated at 200 kV. The specific surface area was calculated by Brunauer-Emmett-Teller (BET) method. Basic strength of the catalysts was measured by Hammett indicator method [15] using phenolphthalein (H_9.8), 2, 4-dinitroaniline (H_15) and 4-nitroaniline (H_18.4) as indicators. Typically, about 100 mg of the CaO was dispersed in 10 mL of a solution of Hammett indicator diluted with methanol and allowed to equilibrate for 2 h. After the equilibration, the color of catalyst was noted. Infrared spectrophotometer (200 FT-IR, Perkin Elmer) was used to identify surface molecular groups of the catalysts and study the interaction between CaO nanopartices and methanol (calcium methoxide) or glycerol (calcium diglyceroxide). Calcium methoxide were prepared in colloidal form by dispersion of nano CaO in methanol using ultrasonic bath and then stirred at room temperature for 15 min. After filtration, the obtained sample was dried under nitrogen. Calcium diglyceroxide were produced by stirring the mixture of nanoCaO, methanol and glycerol at room temperature for 15 min. The obtained colloidal suspension was filtered and dried under nitrogen atmosphere.

2.4 Transesterification of Crude Palm Oil

Transesterification reaction was carried out at 60°C in batch reactor that consists of 3-necked round-bottom flask equipped with a reflux condenser. Typically, 30 mL of crude palm oil and colloidal dispersion of CaO catalyst in methanol was added in the reactor. The reaction was conducted under condition of various wt. % of catalysts with methanol to oil ratios of 8:1. The mixture was heated for the required reaction time. In the end, the reaction's product was transferred into glass tube and allowed to settle. The excess methanol on the top layer and glycerol on the bottom layer was separated out using pipette. The remaining oil was washed with hot water several times until the washing becomes clear. The percentage of triglyceride conversion into methyl ester was determined by ^1H NMR spectroscopy. The percentage conversion of methyl ester (% C_{ME}) was estimated according to equation (1) [16].

$$C_{ME} = 100 \times \frac{2 \times I_{ME}}{3 \times I_{CH_2}} \qquad (1)$$

I_{ME} = integration value of the methoxy protons of methyl ester at 3.622 ppm

I_{CH2} = integration value of of a-CH_2 protons at 2.240 ppm

3. RESULTS AND DISSCUSSION

3.1 Synthesis and Characterization of Nano CaO

Nano CaO was prepared through calcination of nano $Ca(OH)_2$ at 700°C. Nano $Ca(OH)_2$ was synthesized in the presence of $Ca(NO_3)_2.4H_2O$ as precursor in ethylene glycol under basic condition. PVP polymer was also used as a stabilizer to protect $Ca(OH)_2$ from aggregation. This stabilizer can be removed during the calcination process. The TEM image of CaO nanoparticles showed a spherical in shape with the average particle size of 12±4 nm (Figure 1a and 1c). In comparison, lab-grade CaO prepared by calcination of $CaCO_3$ has much larger particle size (more than 10 times) and some aggregation can be clearly seen (Figure 1b and 1d).

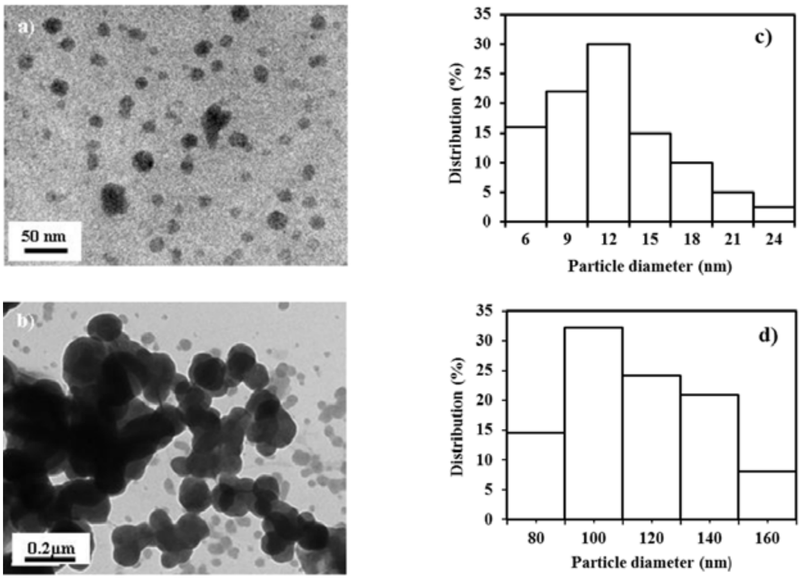

Figure 1. TEM image of a) nano CaO b) Lab-grade CaO c) and d) histogram of the particle size distribution.

XRD pattern of both nano and lab-grade CaO (Figure 2) showed characteristic peaks at $2q$ = 32.1, 37.3, 53.9, 64.1 and 67.3 corresponded to (111), (200), (220), (311) and (222) crystal plane, which are in good agreement with the standard JCPDS file No. 037-1497 for cubic crystal structure. Some minor reflections (less than 5%) is attributed to $Ca(OH)_2$ due to the exposure of CaO to air.

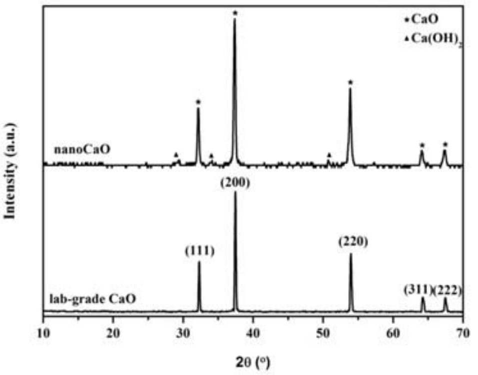

Figure 2. XRD pattern of nano CaO compared with lab-grade CaO.

3.2 Surface Area, Surface Structure and Surface Basicity of CaO Catalyst

A large surface area of nanoparticles can facilitate the access of reactant molecules to basic sites on the catalyst surface. From the Brunauer-Emmett-Teller (*BET*) measurements, the synthesized nano CaO has high surface area of 70.30 m^2g^{-1} while has only 12 m^2g^{-1} of the lab-grade sample. In this case, the extensively high surface areas of nano CaO may serve as an effective catalyst for adsorbing triglycerides and increase interaction between triglyceride and methanol leading to enhance the overall reaction rate of transesterification during biodiesel production [17]. In addition, basicity is very important properties which determined the catalytic activity of solid-based catalysts. This work, basic strength of CaO was determined by Hammett indicator method. High basic strength in the range of 15.0-18.4 was obtained on the synthesized nano CaO. Basic sites of CaO are believed to locate on oxygen (O) atoms because of its ability to interact attractively with a proton [18]. Many studies have shown that the reactivity of oxide surfaces is strongly influenced by the presence of low coordination sites and oxide ion vacancy [19-20]. Oxide ions at low coordination sites (corner and edge sites) play a major role in adsorption and catalytic properties of CaO. Photoluminescence spectroscopy is a highly sensitive technique that can provide information on oxide ions at low coordination sites [21, 22]. Room temperature PL spectra of colloidal nano CaO and lab-grade CaO in aqueous medium are shown in Figure 3.

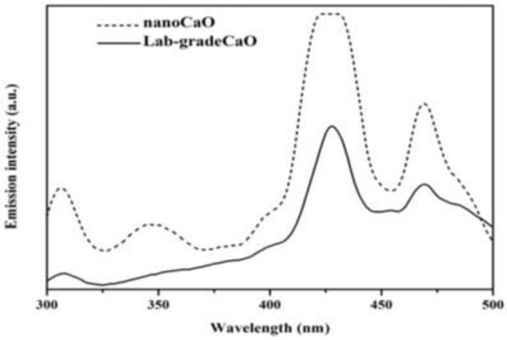

Figure 3. Room temperature PL spectra of colloidal nano CaO and lab-grade CaO excited at 280 nm.

Photoluminescence spectra in Figure 3 showed emission band at 340, 430 and 475 nm which are assigned to five-coordinated terrace (O^{2-}_{5c}), low coordination $O^{2-}_{4c,}$ and O^{2-}_{3c} on edge and corner sites, respectively. This result is consistent with previous reports of Petitjean and co-workers [23] that photoluminesence of CaO powders exhibited emission bands at 350, 395 and 490 nm for excitation wavelengths 250, 285 and 320 nm, respectively, which are assigned to O^{2-}_{5c} $O^{2-}_{4c,}$ and O^{2-}_{3c}, respectively. Higher emission intensity of nano CaO implied higher number of oxide ions at low coordination sites.It is possible that the higher oxide ions at low coordination sites leading to the higher the protonation ability toward methanol and the higher basic reactivity in biodiesel conversion.

3.3 Formation of Methoxide Species

The deprotonation ability of nano CaO toward methanol was identified by the formation of methoxide species. In this study, calcium methoxide (CH_3OCa-OH) was prepared via the dispersion CaO in methanol. Infrared spectra of adsorbed nano calcium methoxide compared to lab-grade are shown in Figure 4. The spectrum of nano CaO showed a sharp stretching peak at 3648 cm^{-1} attributed to structural OH groups adsorbed on CaO surfaces and a broad band centered at 3368 cm^{-1} attributed to adsorption of water. The formation of calcium methoxide can be confirmed by characteristic peaks of -C-H stretching centered at 2839 cm^{-1}, -C-H bending at 1457 cm^{-1} and -C-O stretching at 1081 cm^{-1}. The results are in accordance with previously reported [24]. It is interesting that sharp peaks at 2097 and 2592 cm^{-1} can be noticed only in the nano CaO sample. A peak at 2097 cm^{-1} is assigned to the adsorbed CO generated from methanol oxidation at low-coordinated sites of nano CaO [25] while another peak at 2592 cm^{-1} is attributed to the vibrational frequency of -OH stretching of molecular formic acid adsorbed on the CaO surfaces [26]. A much stronger intensity of -C-H stretching of methoxide species and the formation adsorbed CO peaks implied that the synthesized nano CaO has higher surface areas associated with low coordination sites (edges and corners) and defects on the surfaces. This results lead to a higher activity to methanol deprotonation.

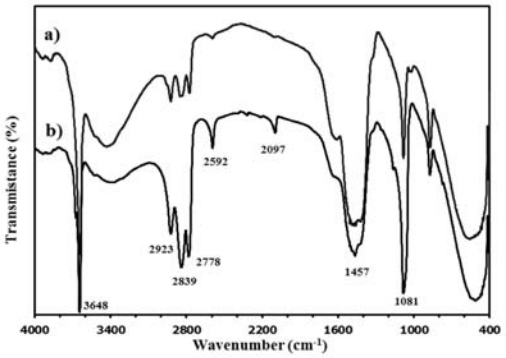

Figure 4. FT-IR spectra of calcium methoxide prepared from a) lab-grade CaO b) nano CaO.

Most importantly, nano CaO is also very sensitive and easier generate surface hydroxyl and carbonyl group in the presence of moisture and CO_2 in air. Therefore, phase changing is an important issue that researchers should be concerned. Many studies have been reported that the order of basic strength is $CaO>Ca(OH)_2>CaCO_3$ [27]. Petitjean and co-workers clearly demonstrated that the hydroxylation level of CaO plays an important role in catalysis and pointed out that this level must be low enough to keep CaO phase and avoid the formation of $Ca(OH)_2$, but high enough to have many surface hydroxyl groups (OH_{ads}) [23]. High population of the low coordination sites (edges and corners) leads to higher surface density of OH groups resulting in higher basic reactivity. Kawashima and co-workers activated CaO by pretreatment with methanol at room temperature for 1 h. Only small amount of CaO was converted into calcium methoxide [28]. However, there has been known that adding a small amount of water to form surface OH, the OH^- will extracts H^+ from methanol to generate methoxide anion and H_2O [29]. However, it should be noted that water containing in reaction leading to the formation of $Ca(OH)_2$ which strongly active with free fatty acid to form calcium soap.

3.4 Transesterification of Crude Palm Oil

Since methanol is very reactive to nano CaO and calcium methoxide was already proved to form at room temperature (30°C), thus in this experiment, transesterification reaction was initially carried out by dispersion nano CaO in methanol before mixing with the palm oil. When heating the mixture at 60°C, color change from yellow to orange can be noticed. After completion of reaction time, the obtained orange suspension was allowed to settle until the separation of layers clearly seen as shown in Figure 5. The yellow layer at bottom is free glycerin and white emulsion at the middle is assigned as soap scum (Ca^{2+}-soap). The orange oil at the top is fatty acid methyl ester (FAME) or biodiesel.

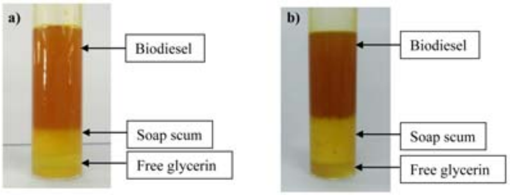

Figure 5. Separated layers from transesterification of crude palm oil using a) nano CaO b) lab-grade CaO.

Biodiesel production from transesterification of crude palm oil using basic catalysts is still limited due to the concurrent soap formation from saponification reaction of contaminant free fatty acid and moisture. Using nano CaO catalyst, clear orange color of biodiesel with less soap emulsion was obtained (Figure 5a) compared with the product obtained from lab-grade CaO (Figure 5b). The excessive amount of soap formed significantly interfered with the washing process by forming emulsions, leading to substantial yield losses. In this study, transesterification of crude palm oil was studied at different reaction times with different wt. % of the synthesized nano CaO. The results of biodiesel production were reported in % FAME and % yield of biodiesel based on mass of palm oil. The results are shown in Table 1.

Table 1. The percentage of biodiesel production from transesterification of crude palm oil using nano CaO compared to lab-grade CaO catalysts.

Catalysts	Wt. %	Reaction time	% FAME*	% yield*
Nano CaO	1	30	90±2	67±2
	1	60	95±2	65±2
	2	15	90±2	65±2
	2	30	98±2	65±2
	2	60	98±2	65±2
	3	60	98±2	65±2
Lab-grade CaO	3	60	65±2	50±3

*% yield of biodiesel is based on mass: (mass of dried biodiesel/ mass of oil used) ×100%, theoretical yield of biodiesel is 70%.

These results clearly demonstrated that nanoscale CaO is an efficient catalyst for transesterification of crude palm oil and has greatly catalytic activity than lab-grade CaO. Under the studied condition, high % FAME and high % biodiesel yield can be achieved. At the reaction temperature of 60°C, the ratio of oil to methanol of 1:8 and 2% of CaO nanocatalyst, up to 98% FAME was obtained only in 30 min. The experiment yield was also close to the theoretical yield of biodiesel (70%). This implied the low formation of soap from saponification reaction. In addition, the separation of glycerin at the bottom was observed immediately, clearly demonstrated complete / almost complete transesterification reaction without or less of diacylglycerol, monoacylglycerol prevented the separation process. Once the biodiesel was separated from the other products and washed with water, some emulsion at interface between oil and water can be observed. This may due to a CaO-glycerin complex that still existed in biodiesel. A CaO-glycerin can be separated by washing with hot water or adding a few drops of citric acid [8].

3.5 Formation of Calcium Diglyceroxide and Catalytic Performance of Nano CaO

Recently, calcium diglyceroxide, $Ca[O(OH)_2C_3H_5]_2$ has been reported as an active species in transesterification of oil [30]. In order to study the formation of calcium diglyceroxide, the experiment was performed by immersing nano CaO in a mix solution of methanol and glycerol at room temperature. FT-IR spectra of the prepared calcium diglyceroxide sample and pristine glycerol are shown in Figure 6. The spectra are in accordance with previously reported [31]. A broad band centered at about 3400 cm^{-1} can be assigned to O-H stretching vibration. The spectra of calcium diglyceroxide and glycerol are similar except some additional peaks can be noticed. A sharp peak at 3,648 cm^{-1} and a small peak at 2841 cm^{-1} are associated to structural OH groups adsorbed on CaO surfaces and C-H stretching of methoxide group, respectively. The formation of methoxide on the surface of calcium diglyceroxide is supposed due to OH groups of glyceroxyl anion promoted adsorption of methanol owing to the attractive intermolecular forcing causing hydrogen bond. The adsorbed methanol is easy to get access to the catalytic sites [32]. Thus, calcium methoxide glyceroxide is proposed as another active species for transesterification of oil. With high low coordination sites, nano CaO is very active to form these active alkoxide species at room temperature.

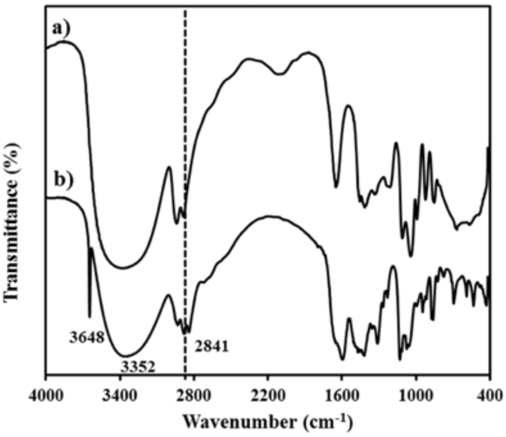

Figure 6. FT-IR spectra of a) glycerol b) calcium diglyceroxide.

CaO is more soluble in glycerol-methanol and biodiesel-glycerol-methanol mixtures compared to that in methanol [33]. The larger solubility of CaO in glycerin mixture was attributed to the formation of calcium diglyceroxide. Transesterification of crude palm oil containing high free fatty acid content, the acidity of the oil may enhance deprotonation of glycerol. Therefore, the strong basicity of oxide ions in low coordination sites of nano CaO combined with the acidity of crude palm oil may play a significant role in promoting high calcium-diglyceroxide formation. However, high acidity of crude palm oil may cause leaching of CaO when the acid amount exceeded a certain percentage. In this study, only small amount/without CaO remains sediment at the bottom of flask after transesterification reaction. In addition, Ca-glycerin complex is highly dispersion in biodiesel fraction causing increase viscosity and form emulsion when washing with water. In this case, high formation of calcium diglyceroxide may intimidate the separation, reusability and the environment sustainability of the catalyst.

In this study, several hypotheses can be proposed to explain the activity and selectivity of CaO nanocatalyst on the production of biodiesel. Firstly, high catalytic activity of nano CaO may due to its high specific surface areas and oxide ions at low coordination sites that can promote the formation of methoxy species at room temperature. Strongly active oxide ions at low coordination sites can directly extract H^+ from the hydroxyl group of methanol to form surface calcium methoxide while bulk CaO requires a small amount of water to activate surface hydroxyl species. Oxide ions at low coordination are also very reactive to moisture to form surface hydroxyl groups which play an important role in its basic reactivity [23]. Secondary, oxide ions at low coordination sites of nano CaO are not only reactive to methanol but also strongly reactive with glycerol to form calcium diglyceroxide. In addition, hydroxyl groups in calcium diglyceroxide can promote the adsorption of methanol owing to hydrogen bond and nonprotonated O atoms are very active to subtract an H atom from the OH group in methanol, yielding a surface methoxide anion which is proposed to accelerate the transesterification of triglyceride. As nano CaO is highly active to deprotonation of methanol and glycerin to form highly reactive methoxide and diglyceroxide species so, formation of scum soap from the influence of water contaminated in oil can be suppressed. High formation of methoxide and glyceroxide leads to a shift of equilibrium into forward direction, increases rate of conversion. Thus, high selectivity to transesterification can be successfully controlled.

4. CONCLUSION

Nanoscale CaO with the particle size less than 15 nm demonstrated a high population of strong basic sites at low coordination atoms which can accelerate deprotonation of methanol and glycerol to generate highly reactive calcium methoxide and calcium glyceroxide species at room temperature. These active species are the key factors to promote rate of transesterification resulting in a decrease soap formation from saponification. Thus, nano CaO is a promising catalyst for transesterification of high free fatty acid-content oil.

ACKNOWLEDGEMENTS

We gratefully thank Faculty of Science, Burapha University for the financial support and Sooksomboon Vegetable Oil Company Limited, Chonburi, Thailand for supporting of crude palm oil.

REFFERENCES

[1] Leung D.Y.C., Wu X. and Leung M.K.H., *Appl. Energ.*, 2010; **87**: 1083-1095. DOI 10.1016/j.apenergy.2009.10.006.

[2] Atadashi I.M., Aroua, M.K., Raman A.A.A. and Sulaiman N.M.N., *J. Ind. Eng. Chem.*, 2013; **19**: 14-26. DOI 10.1016/j.jiec.2012.07.009.

[3] Keera S.T., Sabagh S.M.El. and Taman A.R., *Fuel*, 2011; **90**: 42-47. DOI 10.1016/j.fuel.2010.07.046.

[4] Refaat A.A., *Int. J. Environ. Sci. Technol.*, 2010; **8**: 203-221. DOI 10.1007/bf03326210.

[5] Isahak W.N.R.W., Ismail M., Jahim J.M., Salimon J. and Yarmo M.A., *Chem. Pap.*, 2011; **66**: 178-187. DOI 10.2478/s11696-011-0125-z.

[6] Marinković D.M., Stanković M.V., Velieković A.V., Avramović J.M., Miladinovie M.R., Stamenković O.O., Veljković V.B. and Jovanovia D.M., *Renew. Sust. Energ. Rev.*, 2016; **56**: 1387-1408. DOI 10.1016/j.rser.2015.12.007.

[7] Chaturvedi S., Dave P.N. and Shah N.K., *J. Saudi Chem. Soc.*, 2012; **16**: 307-325. DOI 10.1016/j.jscs.2011.01.015.

[8] Wan Isahak WNR., Ismail M., Mohd Jahim J., Salimon J. and Yarmo M., *World Appl. Sci. J.*, 2010; **9**: 17-22.

[9] Zhao L., Qiu Z. and Stagg-Williams S.M., *Fuel Process. Technol.*, 2013; **114**: 154-162. DOI 10.1016/j.fuproc.2013.03.027.

[10] Venkat Reddy C.R., Oshel R. and Verkade J.G., *Energy Fuels*, 2006; **20**: 1310-1314. DOI 10.1021/ef050435d.

[11] Tahvildari K., Anaraki Y.N., Fazaeli R., Mirpanji S. and Delrish E., *J. Environ. Health Sci. Eng.*, 2015; **13**: 73. DOI 10.1186/s40201-015-0226-7.

[12] Javidialesaadi A. and Raeissi S., *APCBEE Procedia*, 2013; **5**: 474-478. DOI 10.1016/j.apcbee.2013.05.080.

[13] Vasudevan P. and Briggs M., *J. Ind. Microbiol. Biotechnol.*, 2008; **35**: 421-430. DOI 10.1007/s10295-008-0312-2.

[14] Roy A. and Bhattacharya J., *Micro Nano Lett.*, 2010; **5**: 131-134. DOI 10.1049/mnl.2010.0020.

[15] Mar W.W. and Somsook E., *ScienceAsia*, 2012; **38**: 90-94. DOI 10.2306/scienceasia 1513-1874.2012.38.090.

[16] Gelbard G., Bres, O., Vagas R.M, Vielfaure F. and Schuchardt U.F., *J. Am. Oil Chem. Soc.*, 1995; **72**: 1239-1241. DOI 10.1007/BF02540998.

[17] Zu Y., Liu G., Wang Z., Shi J., Zhang M., Zhang W. and Jia M., *Energy Fuels*, 2010; **24**: 3810-3816. DOI 10.1021/ef100419m.

[18] Saifuddin N., Samiuddin A. and Kumaran P., *Trends Appl. Sci. Res.*, 2015; **10**: 1-87.

[19] Coluccia S., Barton A. and Tench A.J., *J. Chem. Soc. Faraday Trans.*, 1981; **77**: 2203-2207. DOI 10.1039/F19817702203.

[20] Nakamura M., Mitsuhashi H. and Takezawa N., *J. Catal.*, 1992; **138**: 686-693. DOI 10.1016/0021-9517(92)90316-a.

[21] Petitjean H., Krafft J.M., Che M., Lauron-Pernot H. and Costentin G., *J. Phys. Chem. C*, 2011; **115**: 751-756. DOI 10.1021/jp110193k.

[22] Sushko P.V., McKenna K.P., Ramo D.M., Shluger A.L., Sterning A., Stankic S., Muller M. and Diwald O., *ECS Trans.*, 2010; **28**: 67-80. DOI 10.1149/1.3367212.

[23] Petitjean H., Chizallet C., Krafft J.M., Che M., Lauron-Pernot H. and Costentin G., *Phys. Chem. Chem. Phys.*, 2010; **12**: 14740-14748. DOI 10.1039/C0CP00855A.

[24] Masood H., Yunus R., Choong T.S.Y., Rashid U. and Taufiq Yap Y.H., *Appl. Catal. A*, 2012; **425-426**: 184-190. DOI 10.1016/j.apcata.2012.03.019.

[25] Sterrer M., Risse T. and Freund H.J., *Appl. Catal. A*, 2006; **307**: 58-61 DOI 10.1016/j.apcata.2006.03.007.

[26] Truong C.M., Wu M.C. and Goodman D.W., *J. Chem. Phys.*, 1992; **97**: 9447-9453. DOI 10.1063/1.463268.

[27] Kouzu M., Kasuno T., Tajika M., Sugimoto Y., Yamanaka S. and Hidaka J., *Fuel*, 2008, **87**: 2798-2806. DOI 10.1016/j.fuel.2007.10.019.

[28] Kawashima A., Matsubara K. and Honda K., *Bioresour. Technol.*, 2009; **100**: 696-700. DOI 10.1016/j.biortech.2008.06.049.

[29] Liu X., He H., Wang Y., Zhu S. and Piao X., *Fuel*, 2008; **87**: 216-221. DOI 10.1016/j.fuel.2007.04.013.

[30] Leon-Reina L., Cabeza A., Rius J., Maireles-Torres P., Alba-Rubio A.C. and Lopez Granados M., *J. Catal.*, 2013; **300**: 30-36. DOI 10.1016/j.jcat.2012.12.016.

[31] Reyero I., Arzamendi G. and Gandia L.M., *Chem. Eng. Res. Des.*, 2014; **92**: 1519-1530. DOI 10.1016/j.cherd.2013.11.017.

[32] Kouzu M., Tsunomori M., Yamanaka S. and Hidaka J., *Adv. Power Technol.*, 2010; **21**: 488-494. DOI 10.1016/j.apt.2010.04.007.

[33] Sharma Y.C., Singh B. and Korstad J., *Fuel*, 2011; **90**: 1309-1324. DOI 10.1016/j.fuel.2010.10.015.